

World Journal of *Diabetes*

World J Diabetes 2022 February 15; 13(2): 70-128



MINIREVIEWS

- 70 Metabolically healthy obesity: Is it really healthy for type 2 diabetes mellitus?
Wu Q, Xia MF, Gao X
- 85 Role of dipeptidyl peptidase 4 inhibitors in the new era of antidiabetic treatment
Florentin M, Kostapanos MS, Papazafiropoulou AK

ORIGINAL ARTICLE**Clinical and Translational Research**

- 97 Altered spontaneous brain activity patterns in patients with diabetic retinopathy using amplitude of low-frequency fluctuation
Shi WQ, Zhang MX, Tang LY, Ye L, Zhang YQ, Lin Q, Li B, Shao Y, Yu Y

Retrospective Study

- 110 Large-scale functional connectivity predicts cognitive impairment related to type 2 diabetes mellitus
Shi AP, Yu Y, Hu B, Li YT, Wang W, Cui GB

LETTER TO THE EDITOR

- 126 Inflammatory bowel disease and diabetes: Is there a link between them?
Sang MM, Sun ZL, Wu TZ

ABOUT COVER

Associate Editor of *World Journal of Diabetes*, Chin-Hsiao Tseng, MD, PhD, Professor, Department of Internal Medicine, National Taiwan University College of Medicine/National Taiwan University Hospital, Taipei 10015, Taiwan. ccktsh@ms6.hinet.net

AIMS AND SCOPE

The primary aim of *World Journal of Diabetes (WJD, World J Diabetes)* is to provide scholars and readers from various fields of diabetes with a platform to publish high-quality basic and clinical research articles and communicate their research findings online.

WJD mainly publishes articles reporting research results and findings obtained in the field of diabetes and covering a wide range of topics including risk factors for diabetes, diabetes complications, experimental diabetes mellitus, type 1 diabetes mellitus, type 2 diabetes mellitus, gestational diabetes, diabetic angiopathies, diabetic cardiomyopathies, diabetic coma, diabetic ketoacidosis, diabetic nephropathies, diabetic neuropathies, Donohue syndrome, fetal macrosomia, and prediabetic state.

INDEXING/ABSTRACTING

The *WJD* is now abstracted and indexed in Science Citation Index Expanded (SCIE, also known as SciSearch®), Current Contents/Clinical Medicine, Journal Citation Reports/Science Edition, PubMed, and PubMed Central. The 2021 Edition of Journal Citation Reports® cites the 2020 impact factor (IF) for *WJD* as 3.763; IF without journal self cites: 3.684; 5-year IF: 7.348; Journal Citation Indicator: 0.64; Ranking: 80 among 145 journals in endocrinology and metabolism; and Quartile category: Q3.

RESPONSIBLE EDITORS FOR THIS ISSUE

Production Editor: *Lin-YuTong Wang*; Production Department Director: *Xu Guo*; Editorial Office Director: *Jia-Ping Yan*.

NAME OF JOURNAL

World Journal of Diabetes

ISSN

ISSN 1948-9358 (online)

LAUNCH DATE

June 15, 2010

FREQUENCY

Monthly

EDITORS-IN-CHIEF

Lu Cai, Md. Shahidul Islam, Jian-Bo Xiao, Manfredi Rizzo, Michael Horowitz

EDITORIAL BOARD MEMBERS

<https://www.wjgnet.com/1948-9358/editorialboard.htm>

PUBLICATION DATE

February 15, 2022

COPYRIGHT

© 2022 Baishideng Publishing Group Inc

INSTRUCTIONS TO AUTHORS

<https://www.wjgnet.com/bpg/gerinfo/204>

GUIDELINES FOR ETHICS DOCUMENTS

<https://www.wjgnet.com/bpg/GerInfo/287>

GUIDELINES FOR NON-NATIVE SPEAKERS OF ENGLISH

<https://www.wjgnet.com/bpg/gerinfo/240>

PUBLICATION ETHICS

<https://www.wjgnet.com/bpg/GerInfo/288>

PUBLICATION MISCONDUCT

<https://www.wjgnet.com/bpg/gerinfo/208>

ARTICLE PROCESSING CHARGE

<https://www.wjgnet.com/bpg/gerinfo/242>

STEPS FOR SUBMITTING MANUSCRIPTS

<https://www.wjgnet.com/bpg/GerInfo/239>

ONLINE SUBMISSION

<https://www.f6publishing.com>

Retrospective Study

Large-scale functional connectivity predicts cognitive impairment related to type 2 diabetes mellitus

An-Ping Shi, Ying Yu, Bo Hu, Yu-Ting Li, Wen Wang, Guang-Bin Cui

ORCID number: An-Ping Shi 0000-0003-1080-9623; Ying Yu 0000-0002-6537-5159; Bo Hu 0000-0002-1135-0669; Yu-Ting Li 0000-0001-9334-5582; Wen Wang 0000-0001-6473-4888; Guang-Bin Cui 0000-0002-6908-0788.

Author contributions: Shi AP performed the data analysis, wrote the draft, conceived and designed the experiments, and rewrote some paragraphs in the introduction and discussion sections; Yu Y, Hu B, Li YT and Wang W obtained grants, conducted the experiments, and contributed to the writing and revision of the manuscript; Cui GB supervised the project, reviewed and edited the manuscript, and managed the submission process; all authors read, revised, and approved the final version of the manuscript.

Institutional review board

statement: This research program was reviewed and approved by Ethics Committee of Tangdu Hospital.

Informed consent statement:

Written informed consent was obtained from all participants before the experiment began.

Conflict-of-interest statement: We have no financial relationships to disclose.

An-Ping Shi, Ying Yu, Bo Hu, Yu-Ting Li, Wen Wang, Guang-Bin Cui, Department of Radiology, Department of Radiology and Functional and Molecular Imaging Key Lab of Shaanxi Province, The Affiliated Tangdu Hospital of Air Force Medical University (Fourth Military Medical University), Xi'an 710038, Shaanxi Province, China

Corresponding author: Guang-Bin Cui, BMed, Doctor, PhD, Academic Research, Chief Doctor, Chief Physician, Professor, Research Dean, Department of Radiology, The Affiliated Tangdu Hospital of Air Force Medical University, No. 569 Xinsi Road, Xi'an 710038, Shaanxi Province, China. cuibtd@163.com

Abstract

BACKGROUND

Large-scale functional connectivity (LSFC) patterns in the brain have unique intrinsic characteristics. Abnormal LSFC patterns have been found in patients with dementia, as well as in those with mild cognitive impairment (MCI), and these patterns predicted their cognitive performance. It has been reported that patients with type 2 diabetes mellitus (T2DM) may develop MCI that could progress to dementia. We investigated whether we could adopt LSFC patterns as discriminative features to predict the cognitive function of patients with T2DM, using connectome-based predictive modeling (CPM) and a support vector machine.

AIM

To investigate the utility of LSFC for predicting cognitive impairment related to T2DM more accurately and reliably.

METHODS

Resting-state functional magnetic resonance images were derived from 42 patients with T2DM and 24 healthy controls. Cognitive function was assessed using the Montreal Cognitive Assessment (MoCA). Patients with T2DM were divided into two groups, according to the presence (T2DM-C; $n = 16$) or absence (T2DM-NC; $n = 26$) of MCI. Brain regions were marked using Harvard Oxford (HOA-112), automated anatomical labeling (AAL-116), and 264-region functional (Power-264) atlases. LSFC biomarkers for predicting MoCA scores were identified using a new CPM technique. Subsequently, we used a support vector machine based on LSFC patterns for among-group differentiation. The area under the receiver operating characteristic curve determined the appearance of the classification.

Data sharing statement: No additional data are available.

Supported by the National Natural Science Foundation of China, No. 81771815.

Country/Territory of origin: China

Specialty type: Endocrinology and metabolism

Provenance and peer review: Unsolicited article; Externally peer reviewed.

Peer-review model: Single blind

Peer-review report's scientific quality classification

Grade A (Excellent): 0
Grade B (Very good): B
Grade C (Good): 0
Grade D (Fair): 0
Grade E (Poor): 0

Open-Access: This article is an open-access article that was selected by an in-house editor and fully peer-reviewed by external reviewers. It is distributed in accordance with the Creative Commons Attribution NonCommercial (CC BY-NC 4.0) license, which permits others to distribute, remix, adapt, build upon this work non-commercially, and license their derivative works on different terms, provided the original work is properly cited and the use is non-commercial. See: <https://creativecommons.org/licenses/by-nc/4.0/>

Received: August 23, 2021

Peer-review started: August 23, 2021

First decision: December 4, 2021

Revised: December 10, 2021

Accepted: January 6, 2022

Article in press: January 6, 2022

Published online: February 15, 2022

P-Reviewer: Bansal A

S-Editor: Wang LL

L-Editor: A

P-Editor: Wang LYT



RESULTS

CPM could predict the MoCA scores in patients with T2DM (Pearson's correlation coefficient between predicted and actual MoCA scores, $r = 0.32$, $P=0.0066$ [HOA-112 atlas]; $r = 0.32$, $P=0.0078$ [AAL-116 atlas]; $r = 0.42$, $P=0.0038$ [Power-264 atlas]), indicating that LSFC patterns represent cognition-level measures in these patients. Positive (anti-correlated) LSFC networks based on the Power-264 atlas showed the best predictive performance; moreover, we observed new brain regions of interest associated with T2DM-related cognition. The area under the receiver operating characteristic curve values (T2DM-NC group *vs.* T2DM-C group) were 0.65-0.70, with LSFC matrices based on HOA-112 and Power-264 atlases having the highest value (0.70). Most discriminative and attractive LSFCs were related to the default mode network, limbic system, and basal ganglia.

CONCLUSION

LSFC provides neuroimaging-based information that may be useful in detecting MCI early and accurately in patients with T2DM.

Key Words: Connectome-based predictive modeling; Large-scale functional connectivity; Mild cognitive impairment; Resting-state functional magnetic resonance; Support vector machine; Type 2 diabetes mellitus

©The Author(s) 2022. Published by Baishideng Publishing Group Inc. All rights reserved.

Core Tip: Large-scale functional connectivity (LSFC) patterns show unique characteristics. Abnormal LSFC patterns have been observed in patients with dementia or mild cognitive impairment. Patients with diabetes may develop mild cognitive impairment that could potentially progress to dementia. We assessed the applicability of LSFC-related discriminative features to predict the cognitive level of patients with type 2 diabetes mellitus using a connectome-based predictive modeling and support vector machine. We found that the application of these two techniques, based on LSFC patterns, to predict neurocognitive abilities, can complement conventional neurocognitive assessments and aid the management of type 2 diabetes mellitus.

Citation: Shi AP, Yu Y, Hu B, Li YT, Wang W, Cui GB. Large-scale functional connectivity predicts cognitive impairment related to type 2 diabetes mellitus. *World J Diabetes* 2022; 13(2): 110-125

URL: <https://www.wjgnet.com/1948-9358/full/v13/i2/110.htm>

DOI: <https://dx.doi.org/10.4239/wjd.v13.i2.110>

INTRODUCTION

Diabetes is a common and frequently occurring disease in clinical practice. It is a non-communicable disease that has gradually attracted increased attention worldwide, and its incidence is increasing with each passing year[1]. Mild cognitive impairment (MCI) occurs in nearly a quarter of patients with type 2 diabetes mellitus (T2DM) and is related to a significantly increased risk of developing dementia[2-5]. Patients with T2DM may present with deteriorated memory, attention, reactivity, and execution[5]. In a cross-sectional study, Biessels *et al*[2] indicated that cognitive function was up to 0.3-0.5 SD lower than that of healthy controls (HC). T2DM leads to a variety of complications, as well as social health and economic problems[3]. In addition, 8.7% of patients with MCI rapidly progress to dementia each year[4]. In patients with T2DM who have a strong tendency to develop MCI and dementia, elucidating the neural mechanisms underlying cognitive dysfunction may assist in clinical identification and intervention, which can mitigate the progress of MCI. However, the mechanism underlying MCI in patients with T2DM warrants further exploration.

Previous studies using neuroimaging measures including the amplitude of low-frequency fluctuation[6], regional homogeneity[7], and functional connectivity[8,9] have reported potential neurobiological underpinnings in patients with T2DM and MCI. However, most of these studies focused on predetermined regions or networks,

including the default mode network (DMN), frontoparietal network (FPN), *etc*[9-12]. Additionally, most of these studies investigated group-wise differences among healthy participants, patients with T2DM with or without MCI, and patients with MCI alone, which limits the provided cognitive information.

Whole-brain functional connectivity, also known as large-scale functional connectivity (LSFC), presents vast functional interaction information between all pairs of brain nodes, which facilitates individual phenotypic prediction and the elucidation of individual differences in cognitive ability[13,14]. There are robust and reliable patterns of LSFC within several brain networks. Therefore, analyzing LSFC patterns may help elucidate the neural mechanisms underlying MCI. Abnormal LSFC patterns were reported in patients with Alzheimer's disease or MCI[15,16]. Additionally, recent functional magnetic resonance imaging (fMRI) studies have used LSFC to successfully predict individual behavioral and cognitive phenotypes, including psychiatric disorders[17], attention ability[18,19], intelligence ability[13], and treatment outcomes[20]. Zeng *et al*[17] used LSFC to discriminate patients with major depressive disorder from matched HC through machine learning (ML) based on LSFC. Similarly, Li *et al* [21] used ML and LSFC to classify patients with schizophrenia and HC.

Similar to fingerprints, individual LSFC patterns are highly unique and reliable, and could be applicable to the recognition of individual characteristics and cognitive function[13,18]. Therefore, some LSFC patterns could be considered as potential biomarkers for evaluating or identifying T2DM-related MCI. However, few studies have used LSFC combined with ML for assessing T2DM[8]. Thus, this study aimed to predict T2DM-related MCI at an individual level using connectome-based predictive modeling (CPM) and a support vector machine (SVM) combined with LSFC.

MATERIALS AND METHODS

Participants

All participants' informed consent forms were signed before the experiment began. LSFC was examined using resting state (rs)-fMRI data obtained from 42 patients with T2DM and 24 HC at Tangdu Hospital, Xi'an, Shaanxi, China, between October 1, 2016, and December 30, 2018. All participants were native Chinese speakers. T2DM was diagnosed based on the fasting blood glucose test (FBG; ≥ 7.0 mmol/L) and oral glucose tolerance test (2 h blood glucose ≥ 11.1 mmol/L after the test)[22], with the diagnosis being confirmed by clinical endocrinologists. Additionally, we administered the Chinese version of the Montreal Cognitive Assessment (MoCA)[23] and Mini-Mental State Examination (MMSE)[24] to classify the cognitive levels of all participants during this experiment. Trained physicians checked for MCI in patients with T2DM, who were divided into the T2DM-C (MoCA score ≤ 23 or MMSE score < 27 , $n = 16$) and T2DM-NC (MoCA score ≥ 26 or MMSE score ≥ 27 , $n = 26$) groups. A MoCA score ≤ 23 [25] or MMSE score < 27 [24] is indicative of cognitive impairment, whereas a MoCA score ≥ 26 [25] or MMSE score ≥ 27 [24] is considered cognitively normal. The exclusion criteria were as follows: other types of diabetes (type 1 diabetes or gestational diabetes); a history of severe encephalopathy (injury, tumor, inflammation, hemiplegia, or infarction) or myocardial infarction; central nervous system dysfunction or medical diseases that considerably affect neurological function, including acquired immune deficiency syndrome; taking drugs within 3 mo, such as psychoactive and steroid drugs; alcohol or drug addiction; pregnancy; contraindications for MRI examination, including cardiac pacemakers, artificial heart valves, and claustrophobia; body mass index (BMI) >35 kg/m² (because obesity impairs cognition); and unfavorable image quality or lack of coordination (head movement: translation >3.0 mm or rotation in any direction $>3^\circ$). Similar exclusion criteria were adopted for the HC group.

MoCA scores

The MoCA is a quick evaluation scale for screening MCI[23,25]. Compared to the MMSE, the MoCA is more suitable for the screening and monitoring of MCI and dementia[23,25]. In our study, we used the Chinese version of the MoCA Basic (MoCA-BC) to assess the cognition level in patients with T2DM. MoCA-BC is recognized as a reliable test in cognitive screening, especially for milder forms of cognitive impairment across the education of all levels, especially in older Chinese adults, which has higher acceptance and better reliability[26]. It has good standard correlation validity (Pearson correlation coefficient MoCA-BC *vs.* MMSE = 0.787) and credible internal consistency (Cronbach alpha = 0.807)[26]. MoCA is scored on a 30-

point scale and comprises 11 items assessing orientation, attention, calculation, recall, and language. A MoCA score ≤ 23 indicates cognitive impairment and one ≥ 26 is considered to indicate cognitively normal.

Image acquisition and preprocessing

MRI data were obtained using a GE Discovery MR750 3.0T scanner (GE Medical Systems) with a brand-new coil system and high scanning speed. Foam pads were used to minimize head movement and earplugs were used to silence the scanner noise. During the acquisition phase, the participants were asked to relax, including at rest, to close their eyes, not think about anything, not allow being disturbed by others, and not to sleep. We recorded the blood oxygen level-dependent signals of spontaneous fluctuations during wakeful rest to assess brain activity. Three-dimensional brain volume (3D-BRAVO) and blood oxygen level-dependent sequences were used to obtain structural (including high-resolution T1-weighted images) and functional images, respectively. For details regarding the scanning parameters, see the Supplementary Material.

Data processing was conducted using DPABI (<http://www.rfmri.org/>)[27] and SPM (<http://www.fil.ion.ucl.ac.uk/spm/>), as well as homemade codes in MATLAB 2018a (MathWorks, Inc., Natick, MA). For details regarding rs-fMRI data preprocessing, see the Supplementary Material.

Functional connectivity network construction

Figure 1A shows the procedure for constructing functional brain networks. Brain regions were marked using three templates; namely, the Harvard Oxford (HOA-112) atlas[28], Automated Anatomical Labeling (AAL-116) atlas[29], and 264-region functional (Power-264) atlas introduced by Power *et al*[30]. We used the Pearson correlation analysis to calculate the mean time series of any two brain regions. Fisher's *r*-to-*z* transformation was applied to convert correlation coefficients to *z*-values. For each participant, an $N \times N$ (HOA-112 atlas, $n = 112$; AAL-116 atlas, $n = 116$; Power-264 atlas, $n = 264$) symmetric matrix was obtained.

We defined network nodes using the HOA -112, AAL-116, and Power-264 atlases. As previously described[31], 112 nodes were used to divide the brain into eight functional networks and the 116 nodes into nine macroscale brain regions. The eight functional networks included the visual (VN), sensory-motor (SMN), dorsal attention (DAN), ventral attention (VAN), limbic system, FPN, DMN, and basal ganglion (BG) networks. The nine macroscale brain regions included the VN, SMN, DAN, VAN, limbic system, FPN, DMN, BG, and cerebellar networks. Additionally, 264 nodes were divided into 14 Large-scale regions[30]. These nodes belonged to the DMN, salience, Cingulo-opercular Task Control (COTC), Fronto-parietal Task Control (FPTC), DAN, VAN, VN, auditory, Sensory/somatomotor Hand (SSH), Sensory/somatomotor Mouth (SSM) subcortical, Memory retrieval, cerebellar and uncertain networks. Details regarding the three templates can be found in Supplementary Tables 1, 2 and 3, as well as Supplementary Figure 1. Additionally, we calculated the group mean functional connectivity matrices (FCMs) based on the three atlases for all three groups. Pairwise connectivity among the network nodes was described as a two-dimensional matrix using the functional connectivity matrix (FCM). In Supplementary Figure 2, the various regions of high (redder) and low (bluer) synchronization levels represent the FCM patterns of both patient groups, which were complex and similar. However, no evident between-group differences were found in the highlighted areas. Generally, the patient groups had fewer but stronger connections than the HC group.

Feature selection and connectome-based predictive modeling

Machine learning-based classification and prediction can allow the identification of clinically feasible neuroimaging biomarkers for cognitive decline in T2DM patients. We used CPM and SVM to obtain neuroimaging-based information potentially facilitating the clinical diagnosis of T2DM-C. Both analytical methods established links between the LSFC and several behavioral measures to generate a predictive model of behavioral data obtained from LSFC. However, SVM used the participants' group labels (*i.e.*, T2DM-C, T2DM-NC, and HC) as behavioral data while CPM used the MoCA scores in patients with T2DM.

Figure 1B illustrates the key CPM steps. Step 1: For each participant, CPM inputs comprised a set of $M \times M$ FCMs based on three atlases and a set of behavioral measures (here, MoCA scores). In the set of $M \times M$ FCMs, the number of brain regions or nodes is denoted by *M*; moreover, the between-node connection strength is associated with the matrix elements. Step 2 (feature selection): The Pearson's

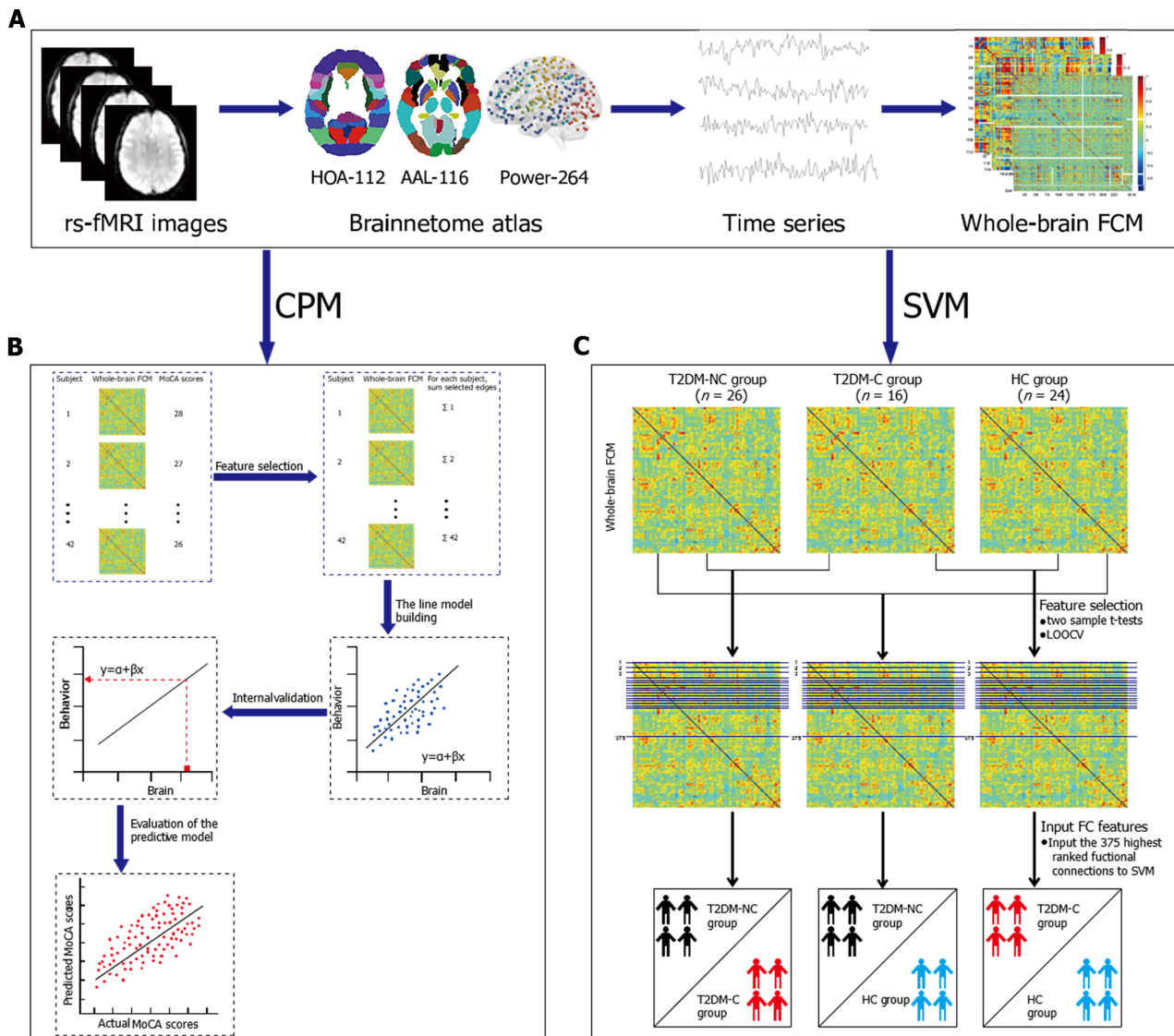


Figure 1 The prediction and classification flowchart. A: Relevant information from image preprocessing to feature identification; B: Detailed steps of connectome-based predictive modeling; C: Detailed steps of support vector machine. rs-fMRI: Resting state functional magnetic resonance imaging; HOA-112: Harvard Oxford atlas; AAL-116: Automated Anatomical Labeling; Power-264: 264-region functional atlas introduced by Power *et al.*; FCM: Functional connectivity matrix; MoCA: Montreal Cognitive Assessment; T2DM: Type 2 diabetes mellitus; T2DM-C/T2DM-NC: Patients with T2DM with the presence/absence of mild cognitive impairment; HC: Healthy controls; LOOCV: Leave-one-out cross validation; FC: Functional connectivity.

correlation of each edge in the FCMs with the MoCA scores was computed. The most significant edges were pitched on by linear regression and subsequently merged into a single value for each participant. Based on the sign of the resultant r values with respect to a threshold of $P < 0.01$, they were separated into positive and negative tails (*i.e.*, positive and negative correlations, respectively, between the edge strength and MoCA scores)[18,32]. Subsequently, the positive and negative network strengths were computed by summing the edge strengths (*i.e.*, Z scores) for all edges in the positive and negative tails, respectively. Finally, we assessed the correlations of the positive and negative network strengths with the MoCA scores. Step 3 (line model building): Next, once the assumption of a linear relationship between the summary value of the connectivity data (independent variable) and the behavioral variable (dependent variable) was true, the predictive model was built; this was done separately for the positive and negative edge sets. Step 4 (prediction of novel participants): For each participant, the positive and negative edge sets were predicted by the behavioral measures. Given the limited sample size, leave-one-out cross validation (LOOCV) was applied separately to training and test data. The training and test datasets comprised $N-1$ and one participant, respectively. Step 5 (evaluation of predictive model): The comparison between the predicted and observed values can effectively evaluate the predictive model. Predictive accuracy was assessed using Pearson correlation analysis of the predicted and actual scores (r predicted-actual). Prediction performance was

assessed using permutation tests.

Feature selection and support vector machine

An SVM model was used to identify LSFC biomarkers for differentiating between the T2DM-NC/T2DM-C, T2DM-NC/HC, and T2DM-C/HC groups. SVM is the most used classification algorithm in ML[33]. For instance, we trained an SVM model using the training dataset to map the set of features of respective labels when given a specific feature (*e.g.*, LSFC) and label (*e.g.*, T2DM and HC). Therefore, given a new dataset, the SVM can be used to predict its label (group). The performance of these models was estimated through LOOCV using measures of accuracy, sensitivity, the receiver operating characteristic (ROC) curve, and the area under the ROC curve (AUC). The use of SVM was dependent on the Statistics and Machine Learning Toolbox in MATLAB 2018a. **Figure 1C** illustrates the detailed steps of SVM. Step 1: For further selection, some lower triangle elements of each FCM were extracted. The feature space spanned $(112 \times 111)/2 = 6216$, $(116 \times 115)/2 = 6670$, and $(264 \times 263)/2 = 34716$ dimensional functional connections for the HOA-112 atlas, AAL-116 atlas, and Power-264 atlas, respectively. Step 2 (feature selection): As reported previously[17,21], the analysis mentioned above was performed *via* two-sample t-tests and LOOCV. Specifically, 66 observations (FCMs with among-group differences) were subdivided into 66 folds. For each fold, the features were ranked in descending order based on the absolute between-group t values, followed by selection of the most discernible connections (from 1 to 375). Step 3 (input the classification features): We input the 375 highest-ranked functional connections into the SVM classifier model trained by LOOCV using the training data. Step 4 (evaluate the appearance of the SVM model using ROC curves and AUC): Sensitivity and specificity refer to the proportion of true positive and negative samples, which are associated with the diagnostic values.

Statistical analysis

SPSS (version 20.0; SPSS, Chicago, IL, USA) was used for statistical analysis. $P < 0.05$ indicated statistical significance. Grouped non-continuous data, including sex, were compared using chi-squared tests. We used one-way analysis of variance to evaluate normally distributed quantitative data, including education, HbA1c (%), BMI, self-rating anxiety scale (SAS) scores, and self-rating depression scale (SDS) scores. The SDS is a simple, 20-question scale that reflects depressive mood, physical symptoms, psychomotor behavior, and psychological symptom experience based on how one feels over the course of a week. Since it is self-administered, the test is widely used and does not require others' participation. The SAS is a self-rating scale containing 20 items (hoping to elicit 20 symptoms) divided into 4 grades. The main evaluation item is the frequency of the occurrence of the defined symptoms. The criteria are: "1" the symptoms occur a little or none of the time; "2" a small part of the time; "3" a lot of the time; "4" most or all the time. The SAS is intended for adults with symptoms of anxiety. At the same time, it has a wider applicability than the SDS. For values with significant among-group differences, the least significant difference was used to perform post hoc comparisons between each group pair. Non-normally distributed continuous quantitative data, including age, FBG, waist-to-hip ratio (WHR), systolic pressure, diastolic pressure, total cholesterol, high-density lipoprotein (HDL) cholesterol, triglycerides, urinary microalbumin, duration of diabetes, MMSE scores, and MoCA scores, are expressed as the median (minimum, maximum). Between-group and among-group differences in non-normally distributed data were evaluated using the Mann-Whitney U test and Kruskal-Wallis non-parametric comparisons, respectively. However, the Kruskal-Wallis test could not perform pairwise comparisons among the three groups, which were performed directly through SPSS version 20.0.

P -values were corrected, and multiple comparison issues were addressed by permutation tests[34] performed by randomly assigning participants to two groups 5,000 times. When regional volume and eigenvector centrality values did not belong to the 95% of the null distribution of permutation tests ($P < 0.05$, corrected), the differences were considered significant. All the analyses mentioned above were performed using MATLAB.

RESULTS

Demographic and clinical characteristics

Table 1 summarizes the clinical and demographic characteristics of the T2DM-NC, T2DM-C, and HC groups. No significant between-group differences were found in age, sex distribution, BMI, blood pressure, total cholesterol, triglycerides, urinary microalbumin, duration of diabetes, SAS scores, and SDS scores. Compared with the T2DM-C group, the T2DM-NC and HC groups had higher levels of education ($P = 0.040$ and $P = 0.015$, respectively), MMSE scores ($P < 0.001$ and $P = 0.002$, respectively), and MoCA scores ($P < 0.001$ and $P = 0.001$, respectively). No significant differences were found in education, MMSE scores, and MoCA scores between the T2DM-NC and HC groups. Furthermore, compared with the HC group, the T2DM-C/NC groups had higher levels of HbA1c ($P < 0.001$), HDL cholesterol ($P = 0.005$, $P = 0.006$), FBG ($P = 0.001$, $P < 0.001$), and WHR ($P = 0.017$, $P = 0.002$, respectively). No significant differences were found in the levels of HbA1c, HDL cholesterol, FBG, and WHR between the T2DM-C/NC groups.

Individualized prediction of T2DM outcome

Based on the fMRI data, we found that the CPM, which was based on positive network strength, could significantly predict the participants' MoCA scores (Pearson's correlation of predicted and observed MoCA scores, $r = 0.32$, $P = 0.0066$ [HOA-112 atlas]; $r = 0.32$, $P = 0.0078$ [AAL-116 atlas]; $r = 0.42$, $P = 0.0038$ [Power-264 atlas]; see **Table 2** and **Figure 2**). However, the predictions were not significant in the negative network model. Compared to the random label ($P < 0.01$), permutation tests (repetition times: 5000) indicated the higher actual classification accuracy.

For the HOA-112 atlas, between-network connectivity in the VAN, DMN, and SMN was crucially involved in predicting the MoCA scores in patients with T2DM. For the AAL-116 atlas, significantly discriminative LSFCs were mainly located across the limbic system, DMN, VN, BG, and cerebellum. For the Power-264 atlas, the most significantly predictive LSFCs were those between the VN and SSH. Overall, highly discriminative LSFCs were mainly located in the DMN, limbic system, BG, and VN.

Network anatomy predicts MoCA scores

Next, we investigated the neuroanatomy of positive MoCA networks. **Figure 3A-C** show a circle plot visualization for edges, which comprises the positive MoCA networks. These figures present the general neurocognitive composition of positive MoCA networks, which are indicative of the advanced descriptions of the brain regions involved. **Figure 3D-F** show glass brain plots displaying the above LSFCs localized in the 3D brain space. These figures indicate that these LSFCs, which were used to predict the differences between MoCA scores, were not located in specific brain regions but distributed throughout the brain.

Individualized classification of T2DM outcomes

Table 3 and **Figure 4** show the ROC curves and AUC values. We selected 375 functional connections using the LOOCV after achieving the highest performance. Although the SVM model did not achieve good performance in three two-category classifications, the highest performance was achieved in discriminating between the T2DM-C/NC groups using the 375 highest-ranked functional connections (HOA-112 atlas: AUC=0.70, specificity = 0.69, sensitivity = 0.73, $P = 0.0144$; AAL-116 atlas: AUC = 0.65, specificity = 0.69, sensitivity = 0.65, $P = 0.0556$; Power -264 atlas: AUC = 0.70, specificity = 0.63, sensitivity = 0.77, $P = 0.0160$).

For the HOA-112 atlas, between-network connectivity in the BG, SMN, and FPN was crucially involved in discriminating between the T2DM-C/NC groups. For the AAL-116 atlas, the most discriminative and attractive LSFCs were located between the limbic system and the BG, as well as between the DMN and cerebellum. For the Power-264 atlas, the most significantly predictive functional connections were between the DMN and FPTC network. Overall, the DMN and BG were crucially involved in differentiating between the T2DM-C/NC groups.

Network anatomy in the classification of T2DM-C and T2DM-NC

Next, we visualized the neuroanatomical location of the network identified by classification (T2DM-C group *vs.* T2DM-NC group). **Figure 5A-C** demonstrate the network identified by classification after grouping the edges into macroscale brain regions. **Figures 5D-F** show glass brain plots displaying the same LSFCs localized in the 3D brain space; these figures indicate that these LSFCs, which were also used to predict

Table 1 Demographic and clinical characteristics of these three groups

Characteristics	T2DM-NC (n = 26)	T2DM-C (n = 16)	HC (n = 24)	P value
Age (yr) ²	51 (34, 65)	54 (39, 67)	49 (26, 59)	0.227
Female/Male	4/22	6/10	9/15	0.153
Education (yr) ¹	12.88 ± 2.55	10.81 ± 2.76	13.38 ± 3.88	0.040
HbA1c (%) ¹	8.13 ± 1.87	9.06 ± 1.77	5.66 ± 0.33	0.000
FBG (mg/dL) ²	7.85 (4.20, 15.80)	7.60 (3.60, 11.70)	5.20 (4.80, 6.80)	0.000
BMI (kg/m ²) ¹	25.26 ± 2.43	24.90 ± 2.97	23.80 ± 2.41	0.779
WHR ²	0.91 (0.76, 0.96)	0.91 (0.86, 0.96)	0.87 (0.78, 0.93)	0.004
Blood pressure (mmHg)				
SP ²	128.00 (105.00, 150.00)	120.00 (101.00, 150.00)	128.00 (100.00, 181.00)	0.836
DP ²	80.00 (60.00, 90.00)	80.00 (60.00, 90.00)	80.00 (67.00, 118.00)	0.432
Total cholesterol ²	4.04 (2.76, 6.69)	4.21 (2.63, 5.71)	4.43 (3.69, 5.39)	0.407
HDL cholesterol ²	1.35 (0.43, 6.60)	1.26 (0.53, 8.08)	0.94 (0.71, 1.64)	0.001
Triglycerides (mg/dL) ²	1.75 (0.43, 6.60)	1.26 (0.53, 8.08)	2.06 (0.87, 6.41)	0.457
UMA (µg/min) ²	12.45 (1.00, 342.70)	15.95 (7.00, 299.00)	13.65 (0.40, 58.60)	0.706
Duration of diabetes (mo) ²	96.00 (0.25, 180.00)	24.00 (0.25, 228.00)		0.515
MMSE ²	29.00 (27.00, 30.00)	26.00 (23.00, 29.00)	28.00 (27.00, 30.00)	0.000
MoCA ²	27.00 (25.00, 30.00)	24.00 (18.00, 30.00)	27.00 (24.00, 30.00)	0.000
SAS ¹	41.62 ± 7.12	43.75 ± 7.26	39.54 ± 7.00	0.190
SDS ¹	46.12 ± 6.87	45.31 ± 8.46	41.71 ± 10.07	0.172

¹Data are presented as mean ± SD.

²Data are presented as median (minimum, maximum).

P < 0.05 was considered significant. T2DM: Type 2 diabetes mellitus; T2DM-C/T2DM-NC: Patients with T2DM with the presence/absence of mild cognitive impairment; HC: Healthy controls; HbA1c: Glycosylated hemoglobin A1c; FBG: Fasting blood glucose; BMI: Body mass index; WHR: Waist-to-Hip Ratio; SP: Systolic pressure; DP: Diastolic pressure; HDL: High density lipoprotein; UMA: Urinary microalbumin; MMSE: Mini-mental state examination; MoCA: Montreal cognitive assessment; SAS: Self-rating anxiety scale; SDS: Self-rating depression scale.

Table 2 Prediction outcome

Brain atlas	Correlation coefficient	P value
HOA-112 atlas	0.32	0.0066
AAL-116 atlas	0.32	0.0078
Power-264 atlas	0.42	0.0038

HOA-112: Harvard Oxford atlas; AAL-116: Automated Anatomical Labeling; Power-264: 264-region functional atlas introduced by Power *et al.*

the differences between MoCA scores, were not located in specific brain regions but distributed throughout the brain.

DISCUSSION

The present study examined whether we could adopt LSFC patterns as discriminative features to classify and predict cognitive impairment related to T2DM with a high degree of accuracy. Compared to neuropsychological scales, which may be unreliable and subjective, it is evident from our results that LSFC is useful in the early detection of MCI related to T2DM. Our results indicate that functional networks contain clinically relevant cognition-related information, which is defined in a data-driven

Table 3 Classification outcome

Group	Brain atlas	AUC	Specificity	Sensitivity	P value
T2DM-NC vs T2DM-C	HOA-112 atlas	0.70	0.69	0.73	0.0144
	AAL-116 atlas	0.65	0.69	0.65	0.0556
	Power-264 atlas	0.70	0.63	0.77	0.0160
T2DM-NC vs HC	HOA-112 atlas	0.54	0.75	0.42	0.3122
	AAL-116 atlas	0.53	0.58	0.54	0.3804
	Power-264 atlas	0.56	0.58	0.58	0.2478
T2DM-C vs HC	HOA-112 atlas	0.54	0.63	0.56	0.3152
	AAL-116 atlas	0.72	0.67	0.75	0.0096
	Power-264 atlas	0.70	0.79	0.63	0.0184
T2DM vs HC	HOA-112 atlas	0.67	0.63	0.69	0.0144
	AAL-116 atlas	0.63	0.58	0.64	0.0444
	Power-264 atlas	0.50	0.50	0.67	0.4898

T2DM: Type 2 diabetes mellitus; T2DM-C/T2DM-NC: Patients with T2DM with the presence/absence of mild cognitive impairment; HC: Healthy controls; AUC: The area under the receiver operating characteristic curve; HOA-112: Harvard Oxford atlas; AAL-116: Automated Anatomical Labeling; Power-264: 264-region functional atlas introduced by Power *et al.*

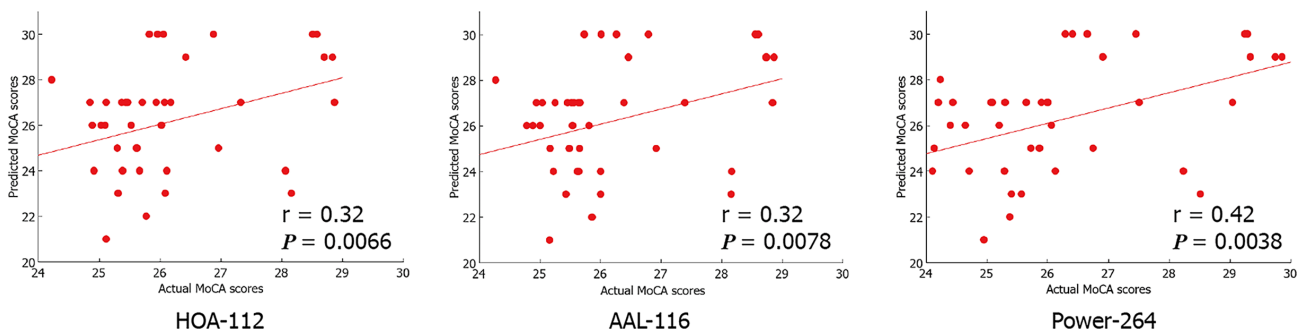


Figure 2 The connectome-based predictive modeling predicted the Montreal Cognitive Assessment scores. Scatterplot of predicted the Montreal Cognitive Assessment (MoCA) scores vs. actual MoCA scores. Predicted scores were derived from edges positively correlated with prediction (positive network). *r*: The *r* value of Pearson's correlation of predicted the MoCA scores and actual MoCA scores; *P*: *P* values from permutation tests (5000 times); T2DM: Type 2 diabetes mellitus; T2DM-C/ T2DM-NC: Patients with T2DM with the presence/absence of mild cognitive impairment; HOA -112: Harvard Oxford atlas; AAL-116: Automated Anatomical Labeling; Power-264: 264-region functional atlas introduced by Power *et al.*

manner and has the potential to be a biomarker to assess the degree of cognitive decline related to T2DM.

T2DM is often associated with cognitive impairment and a higher dementia risk. Patients with T2DM may present with deteriorated memory, attention, reagency, and execution[2-5]. However, the exact pathophysiological mechanisms underlying T2DM-related cognitive dysfunction remain unclear, which impedes the development of preventive treatments. We analyzed resting-state fMRI data using the CPM and SVM. We computed the LSFC patterns using three types of functional brain atlases that separately comprised 112, 116, and 264 nodes covering the whole brain. The SVM-based classification results were not as expected; the exact reasons for which remain unclear. However, the CPM-based prediction results were positive, with exciting prospects. There have been no previous CPM studies on patients with T2DM; moreover, this is the first study to identify LSFC as an imaging biomarker for predicting T2DM-related MCI using CPM. CPM can reliably predict the participants' MoCA scores, which was based on positive network strength ($r = 0.32, P = 0.0066$ [HOA-112 atlas]; $r = 0.32, P = 0.0078$ [AAL-116 atlas]; $r = 0.42, P = 0.0038$ [Power-264 atlas]). Highly discriminative and attractive LSFCs were mainly located within the DMN, limbic system, BG, VN, or across these regions. Our findings suggest that the resting-state LSFC can reveal T2DM-related MCI, which could be more reliable than

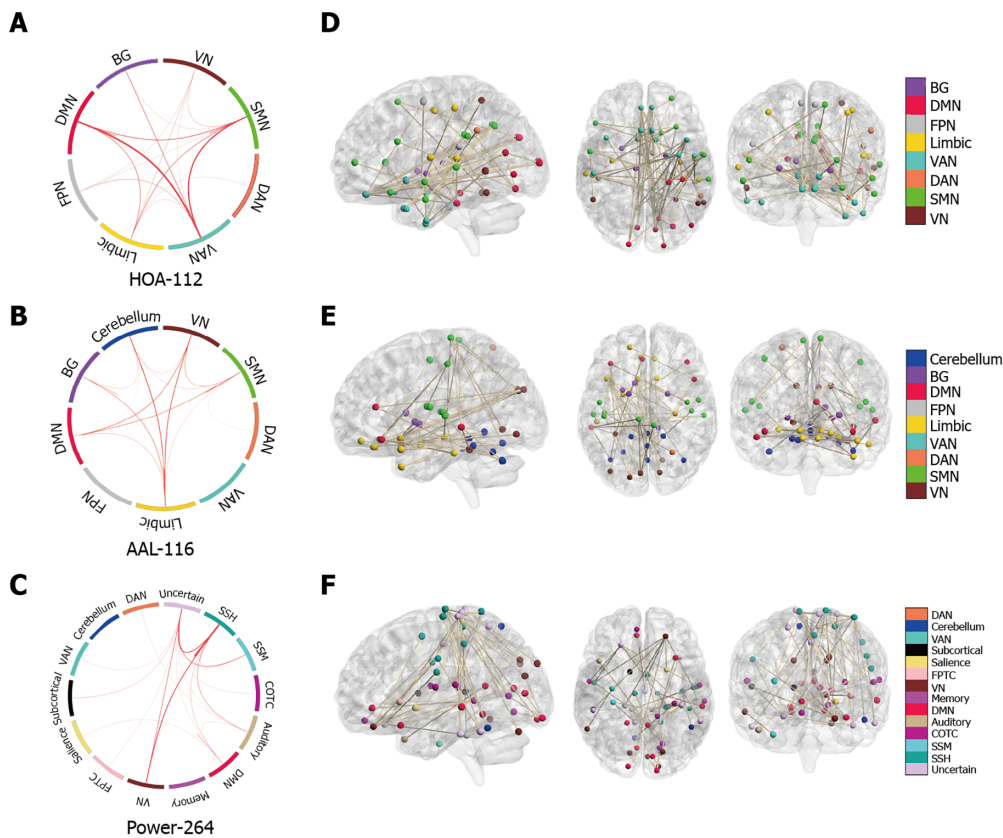


Figure 3 Functional connections predicting individual Montreal Cognitive Assessment scores based on three atlases. A-C: On the far left of the image above, edges were classified as macroscale brain regions, and visualized by circle plots, in which nodes are grouped based on their anatomic location. The resting-state network (RSN) of the brain based on three templates is represented by a rectangle on the circumference of the big circle. The lines connecting two rectangles represent the connections between the corresponding one or two RSNs, including inter-network connections and intra-network connections. The thickness of the line represents the weight (*i.e.*, connectome-based predictive modeling weight) of the connection. The thicker the line, the larger the weight. This visualization was created using CircoS (<http://circoS.ca/>). D-F: On the right of the image above, the same edges are visualized in the brain. The lines represent edges connecting the spheres, which in turn represent nodes. A legend indicating the approximate anatomic 'lobe' is shown in the far right side of the figure. HOA -112: Harvard Oxford atlas; AAL-116: Automated Anatomical Labeling; Power-264: 264-region functional atlas introduced by Power *et al*; VN: Visual Network; SMN: Sensory-motor Network; DAN: Dorsal Attention Network; VAN: Ventral Attention Network; Limbic: Limbic System; FPN: Fronto-parietal network; DMN: Default mode network; BG: Basal ganglia; SSH: Sensory somatomotor hand; SSM: Sensory somatomotor mouth; COTC: Cingulo-opercular task control; Memory: Memory retrieval; FPTC: Fronto-parietal task control.

standardized neuropsychological scales. There is significant interest in using the LSFC to predict human behavior. We found that the LSFC-based CPM could effectively predict the MoCA scores in patients with T2DM. The prediction of neurocognitive abilities from CPM can complete the conventional assessments. The CPM-related positive network was used as a T2DM-related MCI connectivity measure and showed favorable results based on the Pearson correlation coefficient. CPM can predict individual behaviors or characteristics by LSFC, which is novel and data-driven[13,35]; moreover, it can successfully predict the number of psychiatric and psychological phenotypes[32,36]. CPM can isolate brain "fingerprints" that identify individual participants from a group[13], as well as predict personality traits[32], sustained attention[18,37], treatment outcomes[20], and cognitive dysfunction[8,38]. However, unlike previous studies on fluid intelligence[13] and attention[18], where the positive and negative networks showed comparable predictive performance, we found that the negative network showed an unfavorable predictive performance.

Regarding the functional anatomy of the edges, which is most relevant to individual differences in the degree of cognition, we paid more attention to the CPM-positive network. Moreover, lower MoCA scores were associated with higher network strength, indicating more severe cognitive dysfunction. This suggests that the cognitive decline in T2DM patients may involve abnormal connectivity among these different resting-state networks. For both prediction and classification, most significantly discriminative functional connections were related to the DMN, limbic system, and the BG.

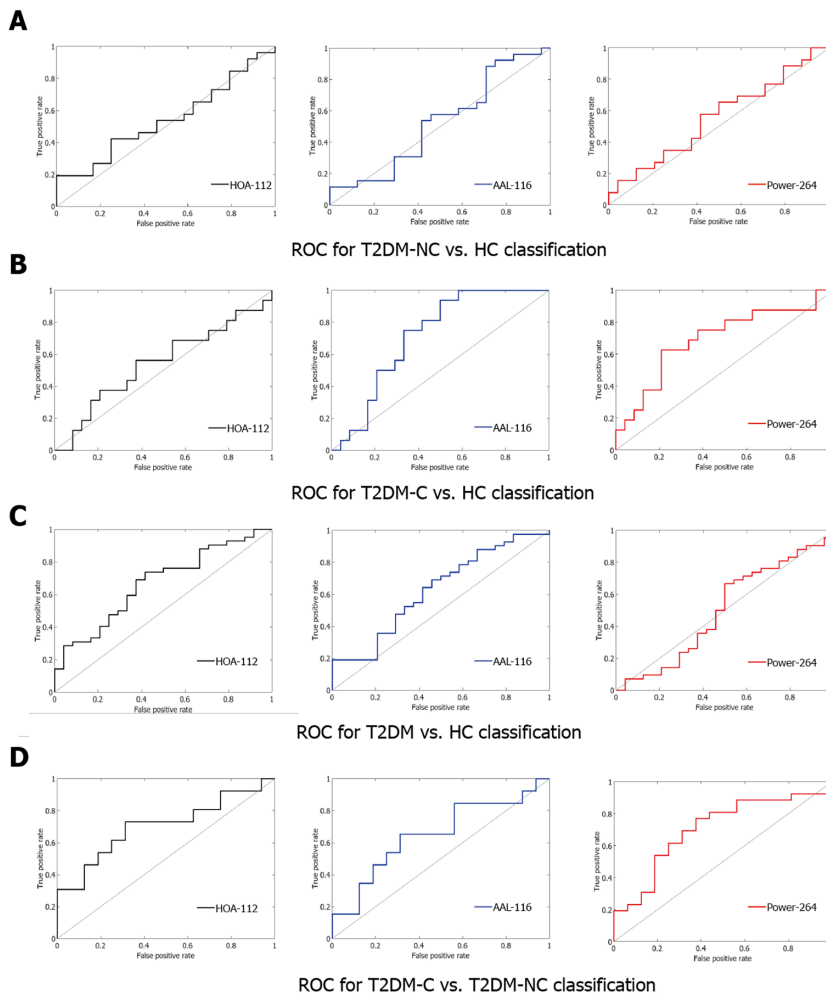


Figure 4 Classification efficiency of support vector machine based on three atlases. The classification effect was not very ideal. A: The area under curve (AUC) value of patients with type 2 diabetes mellitus (T2DM) with the absence of mild cognitive impairment (T2DM-NC) Versus healthy controls (HC) group was 0.54 [Harvard Oxford (HOA-112) atlas], 0.53 [Automated Anatomical Labeling (AAL-116) atlas], 0.56 [264-region functional (Power-264) atlas]; B: the AUC value of patients with T2DM with the presence of mild cognitive impairment (T2DM-C) Versus HC group was 0.54 (HOA-112 atlas), 0.72 (AAL-116 atlas), 0.70 (Power-264 atlas); C: the AUC value of T2DM Versus HC group was 0.67 (HOA-112 atlas), 0.63 (AAL-116 atlas), 0.50 (Power-264 atlas); D: the AUC value of T2DM-C Versus T2DM-NC group was 0.70 (HOA-112 atlas and Power-264 atlas), 0.65(AAL-116 atlas). ROC: receiver operating characteristic curve.

The DMN is activated during wakeful rest and deactivated during cognitive task execution; further, it is involved in cognitive processing[8,11]. The DMN comprises several brain regions, including the anterior cingulate cortex; medial prefrontal cortex; and the medial, lateral, and inferior parietal cortices[39], which are involved in constructing self-related mental simulations, including recalling the past, thinking about the future, and understanding others' perspectives[8,11]. Cognitive impairment in T2DM is related to reduced connectivity in cognition-related networks, most prominently in the DMN[40]. Changes in brain structure and function are associated with the deterioration of cognition; moreover, blood glucose fluctuations (hyperglycemia or hypoglycemia) may be related to T2DM-related brain changes[41]. Repeated hyperglycemia and hypoglycemia can lead to a variety of metabolic and molecular changes that eventually lead to widespread changes in brain cells. However, the exact causes of T2DM-related changes in the DMN are unclear. Specific alterations in functional connectivity may contribute to cognitive decline in patients with T2DM and may represent a promising biomarker.

The cingulate/paracingulate gyrus and parahippocampal gyrus are indispensable to the functioning of the limbic system. They are crucially involved in learning, emotion, memory, and other processes. A recent meta-analysis, including 15 structural studies and 16 functional studies, reported decreased global and regional gray matter volume in the limbic system of patients with T2DM, which could be associated with poor cognitive performance[42]. The results from some studies indicate that the changes in limbic regions, especially in dendritic structures, inhibit the formation of the spinal cord due to the chronic hyperglycemia; moreover, they may also disrupt the

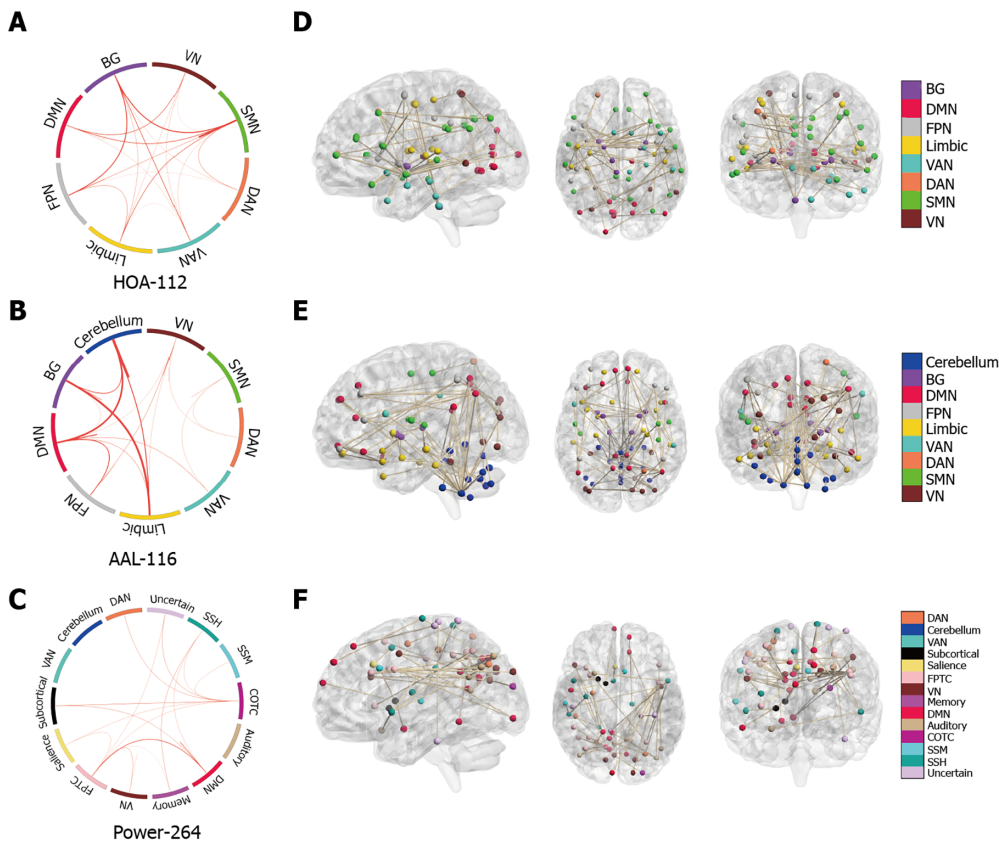


Figure 5 Functional connections classifying patients with type 2 diabetes mellitus with the present of mild cognitive impairment and patients with type 2 diabetes mellitus with the absence of mild cognitive impairment based on three different atlas. A-C: On the far left of the image above, edges were classified as macroscale brain regions and were visualized using circle plots, in which nodes are grouped based on anatomic location. The resting-state network (RSN) of brain based on three atlas is represented by a rectangle on the circumference of the big circle. The lines connecting two rectangles represent the connections between the corresponding one or two RSN, including inter-network connections and intra-network connections. The thickness of the line represents the weight (*i.e.*, support vector classification weight) of the connection. The thicker the line, the larger the weight. This visualization was created using Circos (<http://circos.ca>); D-F: On the right of the image above, the same edges are visualized on brains. The lines represent edges connecting the spheres, which represent nodes. A legend indicating the approximate anatomic 'lobe' is shown in the far right side of picture. VN: Visual network; SMN: Sensory-motor network; DAN: Dorsal attention network; VAN: Ventral attention network; Limbic: Limbic system; FPN: Fronto-parietal network; DMN: Default mode network; BG: Basal ganglia; SSH: Sensory Somatomotor hand; SSM: Sensory somatomotor mouth; COTC: Cingulo-opercular task control; Memory: Memory retrieval; FPTC: Fronto-parietal task control.

processes of memory and learning[43,44]. In addition, multi-timescale variability of abnormal glucose regulation may be associated with poor cognitive function in patients with T2DM, which may be attributed to the gray matter atrophy in the limbic region[45].

Different structures within the basal ganglia, which is involved in movement regulation, play different roles in various diseases. Lesions in the basal ganglia region mainly result in abnormal movement (increased or decreased movement) and changes in muscle tone (increased or decreased). The basal ganglia represent an important neural functional area, closely related to sensory, motor, visual, behavioral and other functions. This area has a high incidence of stroke. Parkinson's disease and Huntington's disease are among the most studied diseases in the area[46]. There is no adequate evidence regarding a relationship between the basal ganglia and T2DM; however, patients with T2DM-C have been shown to have severely impaired overall network efficiency, with decreased lymph node efficiency and connections in multiple regions, including the limbic system and BG[47]. Additionally, a meta-analysis reported reduced overall brain volume and BG atrophy in patients with T2DM[48]. Basal ganglia changes in diabetics typically occur in hyperglycemic osmotic states in older Asian women[49]. Attributable causes of dyskinesia in diabetic patients include hyperglycemia, high viscosity, changes in brain gamma aminobutyric acid metabolism, diabetic angiopathy, and cytotoxic edema. High blood sugar and viscosity can break down the blood-brain barrier, leading to ischemia. Taken together, T2DM-related cognitive impairment may involve abnormal connection patterns across the DMN, limbic system, and BG.

Overall, our study has three main features. First, this is the first study to successfully apply CPM in patients with T2DM for identifying neuroimaging biomarkers associated with cognitive impairment. Second, unlike most previous studies that performed between-group comparisons using *a priori* defined brain regions/networks[8,9,11,40], we performed whole-brain bottom-up analyses. Therefore, our method could facilitate the identification of crucial features for predicting cognitive performance at an individual level. Third, we used three brain templates, namely the HOA-112, AAL-116, and Power-264 atlases, to demonstrate the predictive utility of CPM for determining T2DM-related cognitive impairment from different perspectives. Still, there are some limitations in this study. First, doubling our sample size might have increase the generalizability of our results. Second, we only used rs-fMRI data, whereas other modalities like structural MRI and diffusion-weighted imaging might provide complementary information to improve the quantification of brain networks. Finally, according to our findings, the neurobiological changes of T2DM can be reflected by the resting-state brain network. More in-depth and longitudinal studies are required to elucidate the specific influence on T2DM pathogenesis, especially T2DM-related problems in thought processing.

CONCLUSION

This study used the CPM method to identify LSFC patterns, including connections across the DMN, limbic system, and BG, as potential biomarkers for overall cognitive status in patients with T2DM. LSFC provided neuroimaging-based information that could clinically predict the MoCA scores in patients with T2DM. Applying CPM based on LSFC for predicting neurocognitive abilities can complement conventional neurocognitive assessments and facilitate the management of patients with T2DM.

ARTICLE HIGHLIGHTS

Research background

Whole-brain functional connectivity patterns, or large-scale functional connectivity (LSFC) patterns, are both highly unique and reliable in each individual, and similar to a fingerprint, can identify individual differences in personality traits or cognitive functions. Abnormal LSFC patterns have been found in patients with dementia, as well as in those with mild cognitive impairment (MCI), which predicted their cognitive performance. It has been reported that patients with type 2 diabetes mellitus (T2DM) may develop MCI that could progress to dementia. We assessed the applicability of LSFC-related discriminative features to predict the cognitive level of patients with T2DM using a connectome-based predictive modeling (CPM) and support vector machine (SVM).

Research motivation

Whether machine learning techniques like CPM and SVM could utilize LSFC patterns to predict T2DM-related MCI with a high degree of accuracy remains unclear.

Research objectives

To investigate the utility of LSFC for more accurately and reliably predicting the cognitive impairment related to T2DM.

Research methods

Resting-state functional magnetic resonance images were derived from 42 patients with T2DM and 24 healthy controls. Cognitive function was assessed using the Montreal Cognitive Assessment (MoCA). Patients with T2DM were divided into two groups, according to the presence (T2DM-C; $n = 16$) or absence (T2DM-NC; $n = 26$) of MCI. Brain regions were marked using the Harvard Oxford (HOA-112), automated anatomical labeling (AAL-116), and 264-region functional (Power-264) atlases. LSFC biomarkers for predicting MoCA scores were identified using a new CPM technique. Subsequently, we used the SVM based on LSFC patterns for among-group differentiation. The area under the receiver operating characteristic curve determined the classification appearance.

Research results

CPM could predict MoCA scores in patients with T2DM, indicating that LSFC patterns represent cognition-level measures in these patients. Positive (anti-correlated) LSFC networks based on the Power-264 atlas showed the best predictive performance ($r=0.42$, $P=0.0038$); moreover, we observed new brain regions of interest associated with T2DM-related cognition. The area under the receiver operating characteristic curve values (T2DM-NC group *vs.* T2DM-C group) were 0.65-0.70, with LSFC matrices based on HOA-112 and Power-264 atlases having the highest value (0.70). Most discriminative and attractive LSFCs were related to the default mode network, limbic system, and basal ganglia.

Research conclusions

LSFC provides neuroimaging-based information that may be useful in detecting MCI early and accurately in patients with T2DM and therefore assist with T2DM management.

Research perspectives

Our study provides promising evidence that LSFC can reveal cognitive impairment in patients with T2DM, although further development is needed for clinical application.

REFERENCES

- Dong Y**, Gao W, Zhang L, Wei J, Hammar N, Cabrera CS, Wu X, Qiao Q. Patient characteristics related to metabolic disorders and chronic complications in type 2 diabetes mellitus patients hospitalized at the Qingdao Endocrine and Diabetes Hospital from 2006 to 2012 in China. *Diab Vasc Dis Res* 2017; **14**: 24-32 [PMID: 27941053 DOI: 10.1177/1479164116675489]
- Biessels GJ**, Strachan MW, Visseren FL, Kappelle LJ, Whitmer RA. Dementia and cognitive decline in type 2 diabetes and prediabetic stages: towards targeted interventions. *Lancet Diabetes Endocrinol* 2014; **2**: 246-255 [PMID: 24622755]
- Roberts RO**, Knopman DS, Geda YE, Cha RH, Pankratz VS, Baertlein L, Boeve BF, Tangalos EG, Ivnik RJ, Mielke MM, Petersen RC. Association of diabetes with amnesic and nonamnesic mild cognitive impairment. *Alzheimers Dement* 2014; **10**: 18-26 [PMID: 23562428 DOI: 10.1016/j.jalz.2013.01.001]
- Ma F**, Wu T, Miao R, Xiao YY, Zhang W, Huang G. Conversion of mild cognitive impairment to dementia among subjects with diabetes: a population-based study of incidence and risk factors with five years of follow-up. *J Alzheimers Dis* 2015; **43**: 1441-1449 [PMID: 25159674]
- Kodl CT**, Seaquist ER. Cognitive dysfunction and diabetes mellitus. *Endocr Rev* 2008; **29**: 494-511 [PMID: 18436709 DOI: 10.1210/er.2007-0034]
- Wang ZL**, Zou L, Lu ZW, Xie XQ, Jia ZZ, Pan CJ, Zhang GX, Ge XM. Abnormal spontaneous brain activity in type 2 diabetic retinopathy revealed by amplitude of low-frequency fluctuations: a resting-state fMRI study. *Clin Radiol* 2017; **72**: 340.e1-340.e7 [PMID: 28041652 DOI: 10.1016/j.crad.2016.11.012]
- Qi N**, Cui Y, Liu JC, Yu M, Teng GJ. [Follow-up of resting-state brain function with magnetic resonance imaging in patients with type 2 diabetes mellitus]. *Zhonghua Yi Xue Za Zhi* 2017; **97**: 3057-3061 [PMID: 29081148 DOI: 10.3760/ema.j.issn.0376-2491.2017.39.004]
- Liu Z**, Liu J, Yuan H, Liu T, Cui X, Tang Z, Du Y, Wang M, Lin Y, Tian J. Identification of Cognitive Dysfunction in Patients with T2DM Using Whole Brain Functional Connectivity. *Genomics Proteomics Bioinformatics* 2019; **17**: 441-452 [PMID: 31786312 DOI: 10.1016/j.gpb.2019.09.002]
- Tan X**, Liang Y, Zeng H, Qin C, Li Y, Yang J, Qiu S. Altered functional connectivity of the posterior cingulate cortex in type 2 diabetes with cognitive impairment. *Brain Imaging Behav* 2019; **13**: 1699-1707 [PMID: 30612339 DOI: 10.1007/s11682-018-0017-8]
- Chen Y**, Liu Z, Wang A, Zhang J, Zhang S, Qi D, Chen K, Zhang Z. Dysfunctional organization of default mode network before memory impairments in type 2 diabetes. *Psychoneuroendocrinology* 2016; **74**: 141-148 [PMID: 27611859 DOI: 10.1016/j.psyneuen.2016.08.012]
- Liu H**, Liu J, Peng L, Feng Z, Cao L, Liu H, Shen H, Hu D, Zeng LL, Wang W. Changes in default mode network connectivity in different glucose metabolism status and diabetes duration. *Neuroimage Clin* 2019; **21**: 101629 [PMID: 30573410 DOI: 10.1016/j.nicl.2018.101629]
- Fang F**, Lai MY, Huang JJ, Kang M, Ma MM, Li KA, Lian JG, Wang Z, Yin DZ, Wang YF. Compensatory Hippocampal Connectivity in Young Adults With Early-Stage Type 2 Diabetes. *J Clin Endocrinol Metab* 2019; **104**: 3025-3038 [PMID: 30817818 DOI: 10.1210/je.2018-02319]
- Finn ES**, Shen X, Scheinost D, Rosenberg MD, Huang J, Chun MM, Papademetris X, Constable RT. Functional connectome fingerprinting: identifying individuals using patterns of brain connectivity. *Nat Neurosci* 2015; **18**: 1664-1671 [PMID: 26457551 DOI: 10.1038/nn.4135]
- Jiang R**, Calhoun VD, Zuo N, Lin D, Li J, Fan L, Qi S, Sun H, Fu Z, Song M, Jiang T, Sui J. Connectome-based individualized prediction of temperament trait scores. *Neuroimage* 2018; **183**:

- 366-374 [PMID: 30125712 DOI: 10.1016/j.neuroimage.2018.08.038]
- 15 **Liu Z**, Zhang Y, Bai L, Yan H, Dai R, Zhong C, Wang H, Wei W, Xue T, Feng Y, You Y, Tian J. Investigation of the effective connectivity of resting state networks in Alzheimer's disease: a functional MRI study combining independent components analysis and multivariate Granger causality analysis. *NMR Biomed* 2012; **25**: 1311-1320 [PMID: 22505275 DOI: 10.1002/nbm.2803]
 - 16 **Liu Z**, Zhang Y, Yan H, Bai L, Dai R, Wei W, Zhong C, Xue T, Wang H, Feng Y, You Y, Zhang X, Tian J. Altered topological patterns of brain networks in mild cognitive impairment and Alzheimer's disease: a resting-state fMRI study. *Psychiatry Res* 2012; **202**: 118-125 [PMID: 22695315 DOI: 10.1016/j.psychres.2012.03.002]
 - 17 **Zeng LL**, Shen H, Liu L, Wang L, Li B, Fang P, Zhou Z, Li Y, Hu D. Identifying major depression using whole-brain functional connectivity: a multivariate pattern analysis. *Brain* 2012; **135**: 1498-1507 [PMID: 22418737 DOI: 10.1093/brain/aws059]
 - 18 **Rosenberg MD**, Finn ES, Scheinost D, Papademetris X, Shen X, Constable RT, Chun MM. A neuromarker of sustained attention from whole-brain functional connectivity. *Nat Neurosci* 2016; **19**: 165-171 [PMID: 26595653 DOI: 10.1038/nn.4179]
 - 19 **Yoo K**, Rosenberg MD, Hsu WT, Zhang S, Li CR, Scheinost D, Constable RT, Chun MM. Connectome-based predictive modeling of attention: Comparing different functional connectivity features and prediction methods across datasets. *Neuroimage* 2018; **167**: 11-22 [PMID: 29122720 DOI: 10.1016/j.neuroimage.2017.11.010]
 - 20 **Lichenstein SD**, Scheinost D, Potenza MN, Carroll KM, Yip SW. Dissociable neural substrates of opioid and cocaine use identified via connectome-based modelling. *Mol Psychiatry* 2021; **26**: 4383-4393 [PMID: 31719641 DOI: 10.1038/s41380-019-0586-y]
 - 21 **Li J**, Sun Y, Huang Y, Bezerianos A, Yu R. Machine learning technique reveals intrinsic characteristics of schizophrenia: an alternative method. *Brain Imaging Behav* 2019; **13**: 1386-1396 [PMID: 30159765 DOI: 10.1007/s11682-018-9947-4]
 - 22 **American Diabetes Association**. Diagnosis and classification of diabetes mellitus. *Diabetes Care* 2014; **37** Suppl 1: S81-S90 [PMID: 24357215 DOI: 10.2337/dc14-S081]
 - 23 **Freitas S**, Simões MR, Alves L, Santana I. Montreal cognitive assessment: validation study for mild cognitive impairment and Alzheimer disease. *Alzheimer Dis Assoc Disord* 2013; **27**: 37-43 [PMID: 22193353 DOI: 10.1097/WAD.0b013e3182420bfe]
 - 24 **Li H**, Jia J, Yang Z. Mini-Mental State Examination in Elderly Chinese: A Population-Based Normative Study. *J Alzheimers Dis* 2016; **53**: 487-496 [PMID: 27163822]
 - 25 **Luis CA**, Keegan AP, Mullan M. Cross validation of the Montreal Cognitive Assessment in community dwelling older adults residing in the Southeastern US. *Int J Geriatr Psychiatry* 2009; **24**: 197-201 [PMID: 18850670 DOI: 10.1002/gps.2101]
 - 26 **Chen KL**, Xu Y, Chu AQ, Ding D, Liang XN, Nasreddine ZS, Dong Q, Hong Z, Zhao QH, Guo QH. Validation of the Chinese Version of Montreal Cognitive Assessment Basic for Screening Mild Cognitive Impairment. *J Am Geriatr Soc* 2016; **64**: e285-e290 [PMID: 27996103 DOI: 10.1111/jgs.14530]
 - 27 **Yan CG**, Wang XD, Zuo XN, Zang YF. DPABI: Data Processing & Analysis for (Resting-State) Brain Imaging. *Neuroinformatics* 2016; **14**: 339-351 [PMID: 27075850 DOI: 10.1007/s12021-016-9299-4]
 - 28 **Makris N**, Meyer JW, Bates JF, Yeterian EH, Kennedy DN, Caviness VS. MRI-Based topographic parcellation of human cerebral white matter and nuclei II. Rationale and applications with systematics of cerebral connectivity. *Neuroimage* 1999; **9**: 18-45 [PMID: 9918726 DOI: 10.1006/nimg.1998.0384]
 - 29 **Tzourio-Mazoyer N**, Landeau B, Papathanassiou D, Crivello F, Etard O, Delcroix N, Mazoyer B, Joliot M. Automated anatomical labeling of activations in SPM using a macroscopic anatomical parcellation of the MNI MRI single-subject brain. *Neuroimage* 2002; **15**: 273-289 [PMID: 11771995 DOI: 10.1006/nimg.2001.0978]
 - 30 **Power JD**, Cohen AL, Nelson SM, Wig GS, Barnes KA, Church JA, Vogel AC, Laumann TO, Miezin FM, Schlaggar BL, Petersen SE. Functional network organization of the human brain. *Neuron* 2011; **72**: 665-678 [PMID: 22099467 DOI: 10.1016/j.neuron.2011.09.006]
 - 31 **Schaefer A**, Kong R, Gordon EM, Laumann TO, Zuo XN, Holmes AJ, Eickhoff SB, Yeo BTT. Local-Global Parcellation of the Human Cerebral Cortex from Intrinsic Functional Connectivity MRI. *Cereb Cortex* 2018; **28**: 3095-3114 [PMID: 28981612 DOI: 10.1093/cercor/bhx179]
 - 32 **Hsu WT**, Rosenberg MD, Scheinost D, Constable RT, Chun MM. Resting-state functional connectivity predicts neuroticism and extraversion in novel individuals. *Soc Cogn Affect Neurosci* 2018; **13**: 224-232 [PMID: 29373729 DOI: 10.1093/scan/nsy002]
 - 33 **Bellec P**, Chu C, Chouinard-Decorte F, Benhajali Y, Margulies DS, Craddock RC. The Neuro Bureau ADHD-200 Preprocessed repository. *Neuroimage* 2017; **144**: 275-286 [PMID: 27423255 DOI: 10.1016/j.neuroimage.2016.06.034]
 - 34 **Smith SM**, Vidaurre D, Beckmann CF, Glasser MF, Jenkinson M, Miller KL, Nichols TE, Robinson EC, Salimi-Khorshidi G, Woolrich MW, Barch DM, Uğurbil K, Van Essen DC. Functional connectomics from resting-state fMRI. *Trends Cogn Sci* 2013; **17**: 666-682 [PMID: 24238796 DOI: 10.1016/j.tics.2013.09.016]
 - 35 **Shen X**, Finn ES, Scheinost D, Rosenberg MD, Chun MM, Papademetris X, Constable RT. Using connectome-based predictive modeling to predict individual behavior from brain connectivity. *Nat Protoc* 2017; **12**: 506-518 [PMID: 28182017 DOI: 10.1038/nprot.2016.178]

- 36 **Lake EMR**, Finn ES, Noble SM, Vanderwal T, Shen X, Rosenberg MD, Spann MN, Chun MM, Scheinost D, Constable RT. The Functional Brain Organization of an Individual Allows Prediction of Measures of Social Abilities Transdiagnostically in Autism and Attention-Deficit/Hyperactivity Disorder. *Biol Psychiatry* 2019; **86**: 315-326 [PMID: [31010580](#) DOI: [10.1016/j.biopsych.2019.02.019](#)]
- 37 **Rosenberg MD**, Scheinost D, Greene AS, Avery EW, Kwon YH, Finn ES, Ramani R, Qiu M, Constable RT, Chun MM. Functional connectivity predicts changes in attention observed across minutes, days, and months. *Proc Natl Acad Sci U S A* 2020; **117**: 3797-3807 [PMID: [32019892](#) DOI: [10.1073/pnas.1912226117](#)]
- 38 **Lin Q**, Rosenberg MD, Yoo K, Hsu TW, O'Connell TP, Chun MM. Resting-State Functional Connectivity Predicts Cognitive Impairment Related to Alzheimer's Disease. *Front Aging Neurosci* 2018; **10**: 94 [PMID: [29706883](#) DOI: [10.3389/fnagi.2018.00094](#)]
- 39 **Anticevic A**, Cole MW, Murray JD, Corlett PR, Wang XJ, Krystal JH. The role of default network deactivation in cognition and disease. *Trends Cogn Sci* 2012; **16**: 584-592 [PMID: [23142417](#) DOI: [10.1016/j.tics.2012.10.008](#)]
- 40 **Macpherson H**, Formica M, Harris E, Daly RM. Brain functional alterations in Type 2 Diabetes - A systematic review of fMRI studies. *Front Neuroendocrinol* 2017; **47**: 34-46 [PMID: [28687473](#) DOI: [10.1016/j.yfrne.2017.07.001](#)]
- 41 **Seaquist ER**. The final frontier: how does diabetes affect the brain? *Diabetes* 2010; **59**: 4-5 [PMID: [20040482](#) DOI: [10.2337/db09-1600](#)]
- 42 **Yao L**, Yang C, Zhang W, Li S, Li Q, Chen L, Lui S, Kemp GJ, Biswal BB, Shah NJ, Li F, Gong Q. A multimodal meta-analysis of regional structural and functional brain alterations in type 2 diabetes. *Front Neuroendocrinol* 2021; **62**: 100915 [PMID: [33862036](#) DOI: [10.1016/j.yfrne.2021.100915](#)]
- 43 **Martínez-Tellez R**, Gómez-Villalobos Mde J, Flores G. Alteration in dendritic morphology of cortical neurons in rats with diabetes mellitus induced by streptozotocin. *Brain Res* 2005; **1048**: 108-115 [PMID: [15916754](#) DOI: [10.1016/j.brainres.2005.04.048](#)]
- 44 **Sánchez F**, Gómez-Villalobos Mde J, Juárez I, Quevedo L, Flores G. Dendritic morphology of neurons in medial prefrontal cortex, hippocampus, and nucleus accumbens in adult SH rats. *Synapse* 2011; **65**: 198-206 [PMID: [20665725](#) DOI: [10.1002/syn.20837](#)]
- 45 **Cui X**, Abduljalil A, Manor BD, Peng CK, Novak V. Multi-scale glycemic variability: a link to gray matter atrophy and cognitive decline in type 2 diabetes. *PLoS One* 2014; **9**: e86284 [PMID: [24475100](#) DOI: [10.1371/journal.pone.0086284](#)]
- 46 **Troncoso-Escudero P**, Sepulveda D, Pérez-Arancibia R, Parra AV, Arcos J, Grunenwald F, Vidal RL. On the Right Track to Treat Movement Disorders: Promising Therapeutic Approaches for Parkinson's and Huntington's Disease. *Front Aging Neurosci* 2020; **12**: 571185 [PMID: [33101007](#) DOI: [10.3389/fnagi.2020.571185](#)]
- 47 **Li C**, Zhang J, Qiu M, Liu K, Li Y, Zuo Z, Yin X, Lai Y, Fang J, Tong H, Guo Y, Wang J, Chen X, Xiong K. Alterations of Brain Structural Network Connectivity in Type 2 Diabetes Mellitus Patients With Mild Cognitive Impairment. *Front Aging Neurosci* 2020; **12**: 615048 [PMID: [33613263](#) DOI: [10.3389/fnagi.2020.615048](#)]
- 48 **Moulton CD**, Costafreda SG, Horton P, Ismail K, Fu CH. Meta-analyses of structural regional cerebral effects in type 1 and type 2 diabetes. *Brain Imaging Behav* 2015; **9**: 651-662 [PMID: [25563229](#) DOI: [10.1007/s11682-014-9348-2](#)]
- 49 **Das L**, Pal R, Dutta P, Bhansali A. "Diabetic striatopathy" and ketoacidosis: Report of two cases and review of literature. *Diabetes Res Clin Pract* 2017; **128**: 1-5 [PMID: [28431304](#) DOI: [10.1016/j.diabres.2017.03.008](#)]



Published by **Baishideng Publishing Group Inc**
7041 Koll Center Parkway, Suite 160, Pleasanton, CA 94566, USA
Telephone: +1-925-3991568
E-mail: bpgoffice@wjgnet.com
Help Desk: <https://www.f6publishing.com/helpdesk>
<https://www.wjgnet.com>

